EK2360 Hands-on MEMS Engineering

Mechanical multi-stable optical in-plane switch design

Authors :
Berger, Rikard
Rutz, Nadja
Engman, Alexander
Isachsen, Hilde

August 12, 2024

Contents

1 Design process

The process for designing the MEMS system was to start by selecting an electrostatic actuation mechanism. A comb drive system was chosen with the motivation that it is easier to reach a relatively large displacement as compared to a parallell-plate actuator. Apart from being able to displace the structure by 15 µm in either direction, a comb drive actuator has a very large stable region compared to a parallel plate actuator. A stable region is important, because it must be possible to control the movement of the structure without having any unwanted runaway motion. Since it is a requirement that the device needs to be able to move and stop anywhere between the ± 15 µm positions, it will very important to define a stable region in which the movement can be precisely managed.

The spring system was chosen to consist of folded springs with anchor points on the outside, as this provided great flexibility in adjusting its properties. The spring constant k will be an important parameter as it is responsible for defining the properties of the spring. Apart from having the correct spring constant in the wanted direction, the two unwanted directions will also have to be investigated and designed properly. If this is not managed, lateral stability or transverse motion of the structure will become an issue.

After settling on the specific parts of the system, two basic designs were outlined. These were then designed in COMSOL in order to perform FEM-simulations on the specific properties of interest. All the important properties such as lateral and rotational stability, stable range of the actuator, spring constants and others were simulated. The process for each part of the system included several iterations in which the results were analyzed and the designed adjusted accordingly. Results from these simulations are included in this report and all of the important steps in the design process are described in sufficient detail.

After COMSOL simulations were finished and all of the relevant design-rules were fulfilled, the designs were finalized using AutoCAD and were implemented onto the chip layout provided in the course. The chip provided space for roughly 50 individual devices, which was enough to implement 4-5 copies of the mandatory device designs, as well as several alternative devices.

1.1 Main design

Actuator

The first actuator system design consists of comb drives attached to a movable center beam. The fixed combs were configured in pairs which are mirrored in the plane of movement. The upper and lower combs are stationary and a voltage of maximum 65 V can be applied in order to create an electrostatic potential to the movable centre structure. As the potential is alternated between the upper and lower pairs of combs, the centre beam can be made to move in both directions. The design is presented in figure 1.

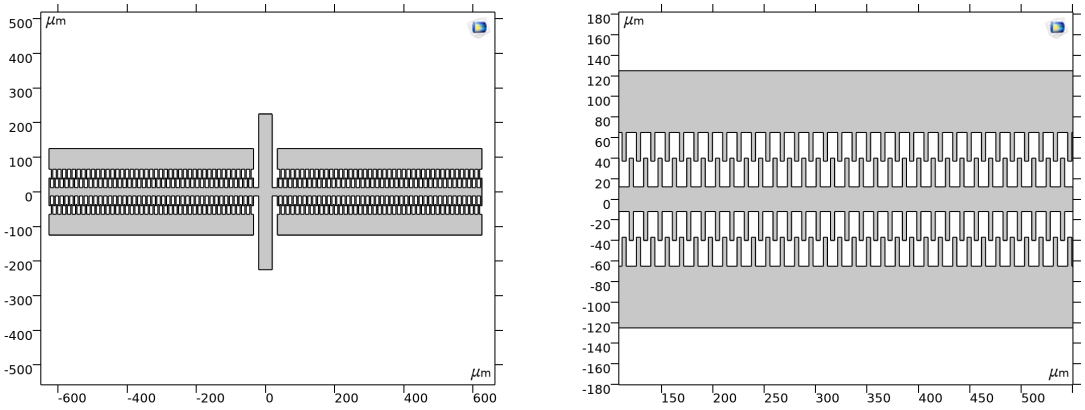

(a) Comb drive configuration.

(b) Comb drive finger specification.

Figure 1: Layout of the main actuator design.

The specifics of the comb drive parameters were calculated using the relation

$$F_{\text{es}} = \varepsilon_0 N \frac{gV^2}{h} \tag{1}$$

where e_0 is the relative permittivity of the medium, in this case air, N is the number of teeth of the comb, g is the spacing between the fingers, V is the applied voltage and h the out-of-plane height of the fingers, in this case 30 µm. This relation was used in order to derive the design parameters of the actuator. The minimum gap allowed of 3 µm was used, which meant that the parameters to simulate were the number of comb fingers and their lengths.

Restoring system

For the restoring mechanism of design I, a symmetrical spring construction was used to optimize stability. The springs and the comb drives will be placed in a symmetrical design. We arrived at the dimensions of the spring by first looking at the dimensions and forces used during the lectures, and then some trial and error. However a much faster way this could or maybe should have been done is by calculating the length from the force and displacement. It would have saved some time in COMSOL, but the extra time plotting this gave us a better understanding of how to use the program.

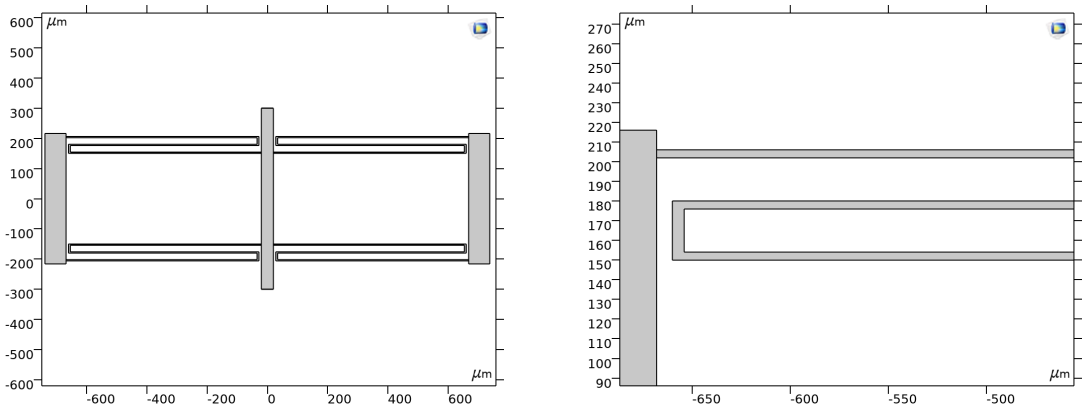

(a) Spring configuration. (b) Spring dimension specification.

Figure 2: Layout of the main restoring mechanism design.

To determine the dimensions of the spring system, the relation

$$k = \frac{EWT^3}{4L^3} \tag{2}$$

was used, in which E is the Young's modulus, W, T and L are dimensional parameters of the spring that can be modified depending on what direction is of importance. The number of folds of the spring also affect the total spring constant.

COMSOL simulations

With electrostatic physics the force was simulated in COMSOL over a displacement ranging from ±15 µm in the x-direction. Over the maximum displacement range it can be seen from the results presented in figure 3 that the comb drive is operating in the constant force region. The constant force is roughly 30±2 µN with 42 fingers on each comb and a finger length of 28 µm. These values were derived from the fact that the maximum dimension of the actuator was 1.5 mm, which added up to roughly 40-45 combs on each actuator when using the smallest allowable dimensions. This determined the maximum force of the displacement, while the finger length determined the length of constant force region.

The lateral stability of the comb drive actuator was also simulated. Since there is a gap of 3 µm between the fingers, it was assumed that the comb drive should be allowed to move maximum 1 µm in the lateral direction to avoid pull-in of the comb fingers. This is however quite conservative as it does not behave as a true parallel plate capacitor. It was then simulated what the lateral displacement and force would be at different insertions of the movable comb. The results are shown in figure 3b which shows the lateral force at different insertions. At a maximum insertion of 15 µm, which is the maximum needed in order for the actuator to fulfill the requirements, the lateral force was 119 $\mathrm{N\,m^{-1}}$, which was taken as the spring constant needed to avoid pull-in.

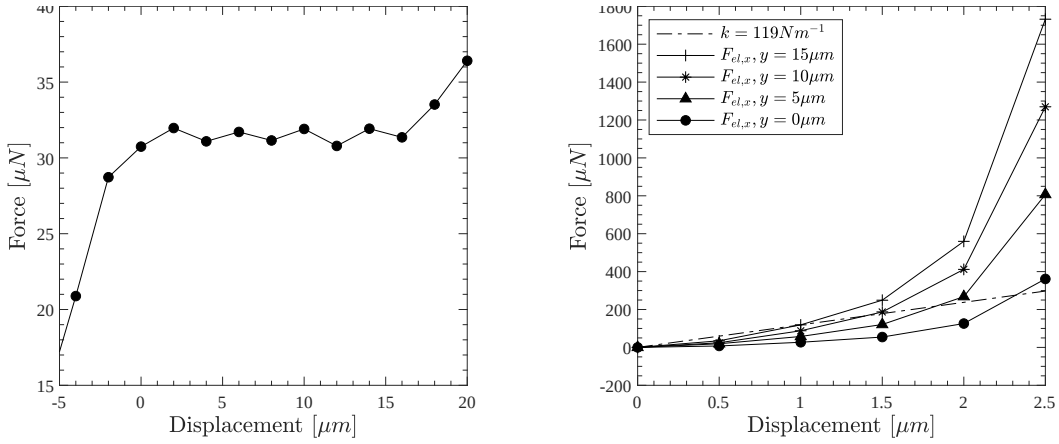

(a) Entire force region (b) Lateral force

Figure 3: Results from simulation of actuator force

The spring system originally provided a spring-constant of $1.74\,\mathrm{N\,m^{-1}}$ in the y-direction and $74.55\,\mathrm{N\,m^{-1}}$ in the x-direction. In order to accommodate for higher demands on the spring constant by the actuator, the system was redesigned. The gap between the springs was decreased from 30 µm to 22 µm. The increase in lateral spring constant should according to equation 2 be $22^3/30^3 \approx 40\%$. After modification, the spring constant was increased to $136.55\,\mathrm{N\,m^{-1}}$ in the unwanted direction while still being able to displace the structure 16.4 µm with a force of 30 µN. This increase was somewhat higher than what equation 2 predicts. The spring constant remained the same in the y-direction after modification, which gives a ratio $k_\mathrm{x}/k_\mathrm{y} = 78$. Simulations of the lateral stability using COMSOL is presented in figure 4.

The rotational stability of the system was also evaluated. The ability of the center structure to counteract rotational movement is important as dimensions are very small. A force of 15.0 µN was applied in the x-direction at the ends of the center structure. This resulted in a movement of 0.912 µm in the x-direction. The rotation was calculated as $rot = \arctan\left(\frac{3.0904\times10^{-6}}{300}\right) = 5.9015 \times 10^{-7}\mathrm{deg}$ and the rotational stability is defined as

$$\frac{LF}{rot} \tag{3}$$

where L is the length of the moving structure and F is the applied force, which in this case gives

$$\frac{2 \times 15 \times 10^{-6} \times 300 \times 10^{-6}}{5.9015 \times 10^{-7}} = 0.0153\,\mathrm{N\,m/deg}$$

.

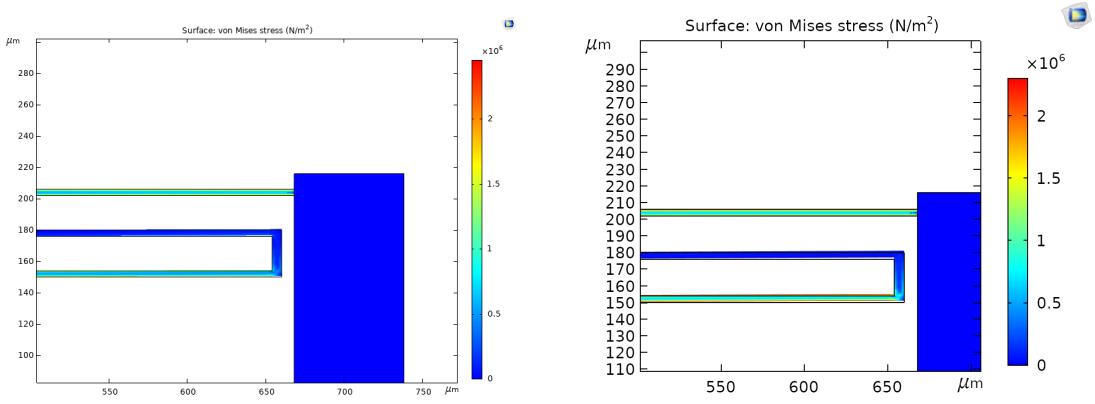

(a) Rotational displacement. (b) Lateral displacement.

Figure 4: Simulation of the main spring design.

1.2 Secondary design

Actuator

The second actuator design is similar to the first designq and has the same number and length of comb fingers and similar dimensions. The main difference is that the combs are not placed on a single center beam structure, but are spaced apart in the xy-plane with respect to each other. This leaves space between the combs to place a spring system. The same parameters of g, N and h were used for this configuration as for the configuration in design I. This also means that the two systems are in essence identical, apart from the relative placement of the combs.

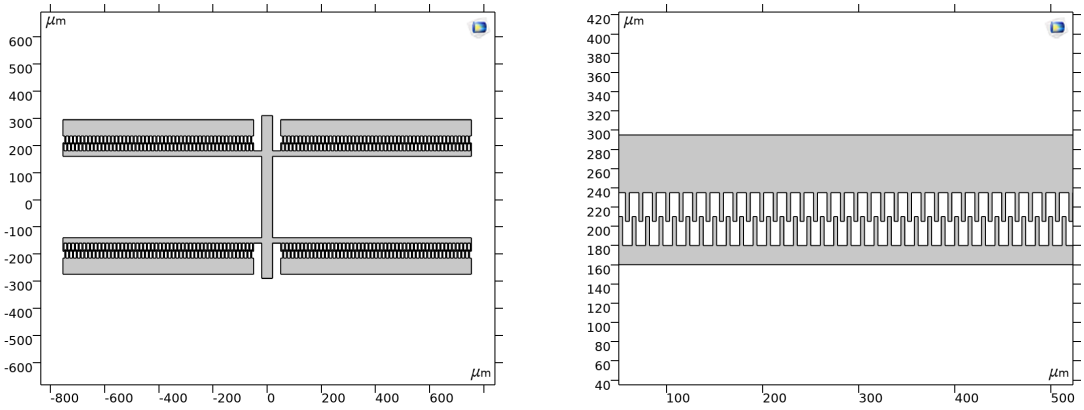

(a) Comb drive configuration. (b) Comb drive finger specification.

Figure 5: Layout of the secondary actuator design.

Restoring system

The restoring system of design the secondary design was adapted from design I to accommodate for the larger spacing between the combs drive actuators. The spring system from the main design was essentially merged into two springs an placed in the center between the actuators. Because the design includes the same parts as the main design, the spring constant is essentially the same in all directions. This means that for lateral stability, both systems will have the same performance. The dimensions of the key parameters such as spring thickness and length are the same as in design I.

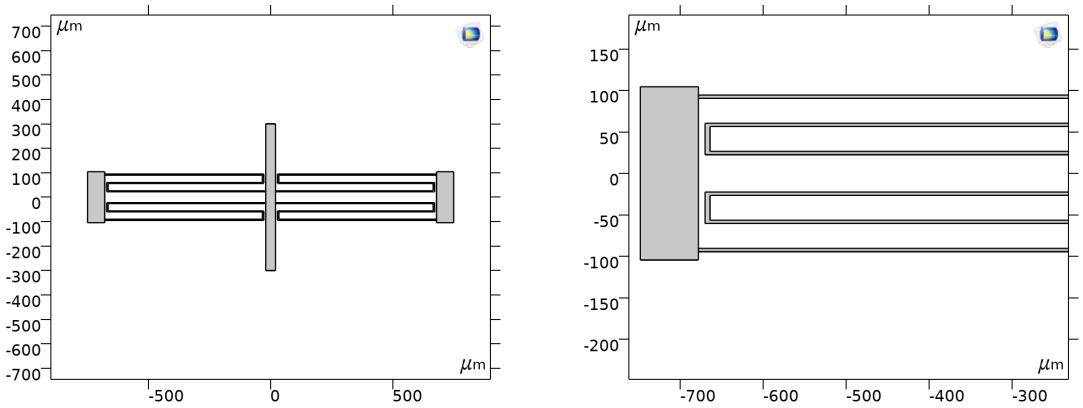

(a) Spring configuration. (b) Spring dimension specification.

Figure 6: Layout of the secondary restoring mechanism design.

COMSOL simulations

The system in the secondary design was evaluated in the same way as the main design. Since the lateral force is independent of the configuration of the actuators, and only depends on their specific geometries, both designs are in this aspect identical, and simulations confirmed the same lateral stability as presented in figure 3. The same applies for the lateral stability of the spring system. The main difference between the designs is the rotational stability. When doing the same evaluation, the system had a rotational stability of 9.218×10^{-9} N m/deg, a factor of 10^6 less than for dthe main design.

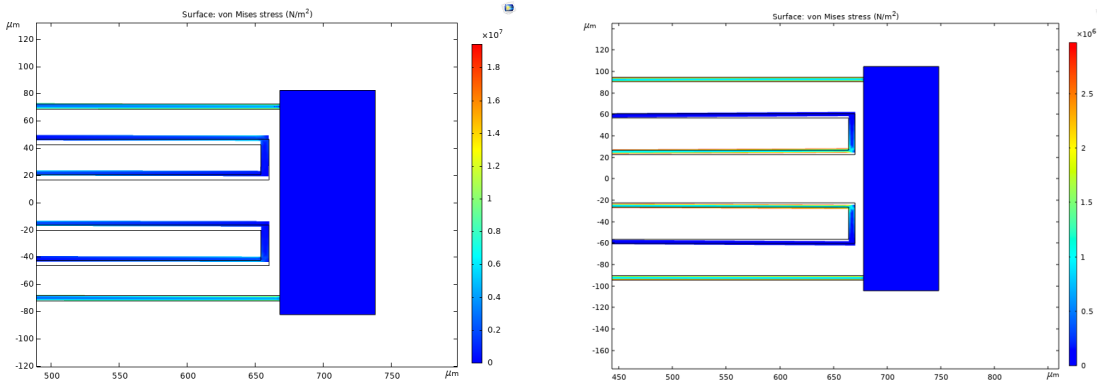

(a) Rotational displacement. (b) Lateral displacement.

Figure 7: Simulation of the secondary spring design.

1.3 Locking mechanism

A locking mechanism consisting of a locking arm which is being actuated by a parallel plate capacitor was chosen. The reason why this design was chosen over a comb drive actuator mechanism was that a large range of motion was not necessary for the locking mechanism to serve its purpose. Thus by designing a parallel plate capacitor actating mechanism, the entire design could be made smaller. The force of a parallel plate capacitor is described by the relation

$$F = \frac{\varepsilon_0 A V^2}{2d^2} \tag{4}$$

where A is the area of the parallel plate, V is the applied voltage and d is the distance between the plates. It is evident that a large force needs a small gap. Thus the smallest allowed gap between the electrode and moving locking mechanism of 3 µm was used. 2 µm was added because there needed to be some overlap of the fingers of the locking mechanism and those of the moving structure. In total it was estimated that 5 µm of movement in the x-direction is necessary in order for the mechanism to be useful.

The force that electrodes of applicable lengths for the design would exert was calculated using equation 4. The electrodes that were simulated had a length of 400 µm, thickness of 4 µm and electrode gap of 4 µm. Electrodes that are larger than those dimensions could not fit on the design or are otherwise not applicable. The electrostatic force was calculated to be roughly 15 µN when using a voltage of 65 V on this setup. This displacement of the locking cantilever was simulated in COMSOL using this force. For a beam of thickness 4 µm, the displacement in the x-direction was 5.4 µm, which was deemed enough for the locking mechanism to fulfill its function.

It was also necessary to simulate if there would be any bending of the cantilever, since it will be rather long and thin and thus act like a spring in the x-direction. When simulating a 500 µm beam with fixed top and bottom points, and a force of 15 µN over the whole cantilever, it moved 8.45 µm at the center point as can be seen in figure 8d. In the simulation, a scale factor of 447 was used to exaggerate the displacement. The stability of the locking mechanism in the direction of the carrier movement was simulated by applying a force of 15 µN to the overlapping area of 2 µm, in order to evaluate whether there would be any large forces and risk of rupture or bending. The results from these simulations can be found in figure 8c. The total displacement of the upper left corner was in the x-direction and in they-direction. All of results from the simulations are acceptable for the intended purpose.

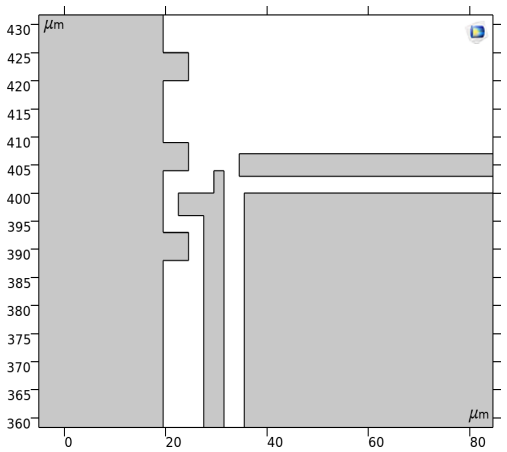

(a) Finalized locking mechanism.

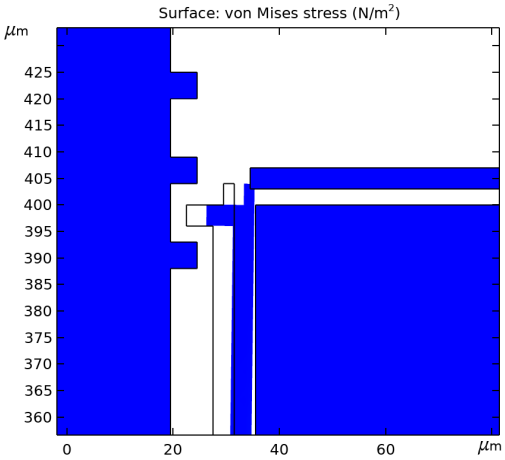

(b) Movement after electrostatic actuation.

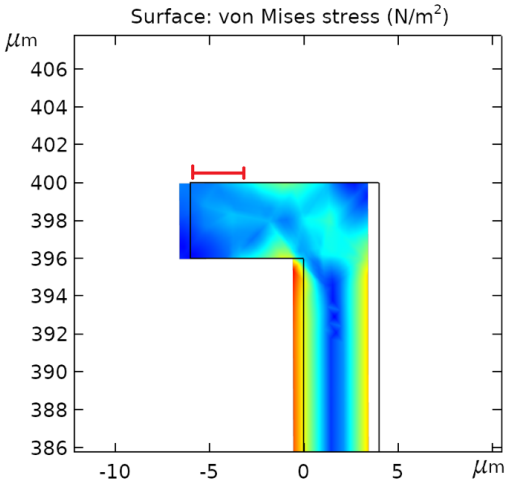

(c) Stability in y-direction

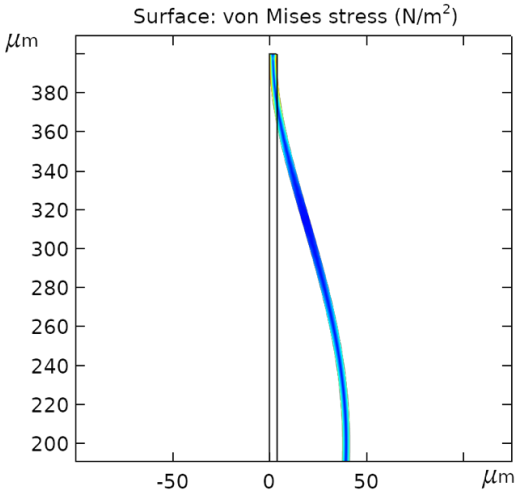

(d) Stability in x-direction.

Figure 8: Figures show properties of the locking mechanism

2 Fabrication

The fabrication process started with a Silicon on Insulator (SOI) wafer. The first step was to spin coat a photoresist onto the wafer. Then, the mask that was produced to include our design was aligned with the wafer and UV light was turned on to pattern the mask onto the wafer. This was a 1:1 ratio mask, which is beneficial when there are as many different designs as on this mask.

Next was the etching of the Si device layer using Deep Reactive Ion Etching (DRIE). This was done using the Bosch process, which flows different gases to get an anisotropic result from an isotropic process. In figure 9 the resulting trenches are displayed after 30 cycles of Si etching. One benefit of using the Bosch process is the ratio achievable between depth and width of an etched hole. Figure 9b displays this well as we have an etch hole that is 47um deep and only 3.31um in diameter.

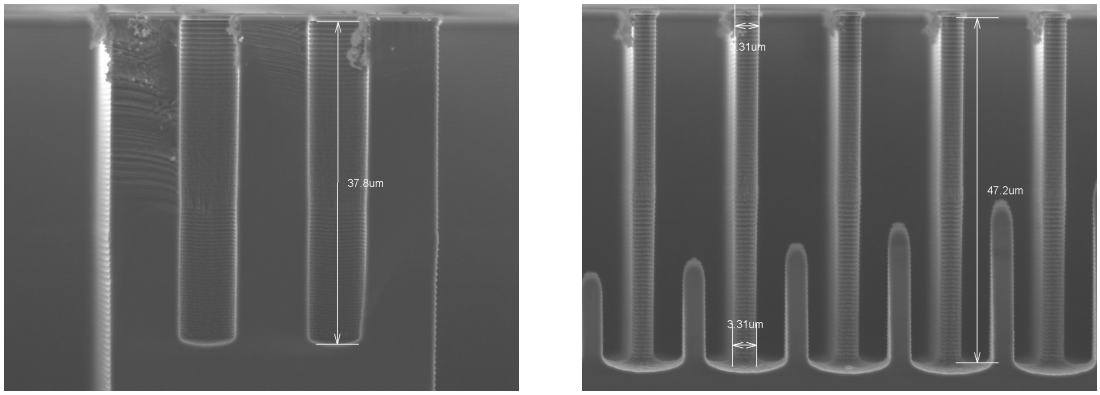

(a) (b)

Figure 9: Cross section of the dummy wafer after 30 cycles of Si etching.

The next step in the fabrication process was dicing the wafer. This had to be done before releasing the structures as it is a much harsher process on the wafer than the rest and would most likely lead to stiction and destruction of devices if done after releasing. Dicing separates each individual chip using a diamond blade. To keep everything in place while dicing the wafer was layered between blue tape.

To release the movable structures, a wet etch of hydrofluoric (HF) acid was used. The chips were in for about three minutes as the etch rate is 1.5nm/min. To make sure the moving structures would not stick to the bottom Si layer, the chips were immediately transferred to isopropanol and then into a Critical Point Dryer (CPD). CPD uses pressure and temperature to avoid the critical point during drying to aviod surface tension forces and stiction of the moving parts.

The last step was metallization. In this step a layer of Aluminum (Al) was deposited onto the chips using sputtering. This step is to have a contact point for the voltage source.

In the images on figure 10 the different parts of the device are viewed using a SEM. It was possible to concentrate the beam on certain parts to confirm movement already at this stage. This can be seen in 10b as the locking mechanism is open and the electrodes are a lighter shade indicating that the beam is concentrated there.

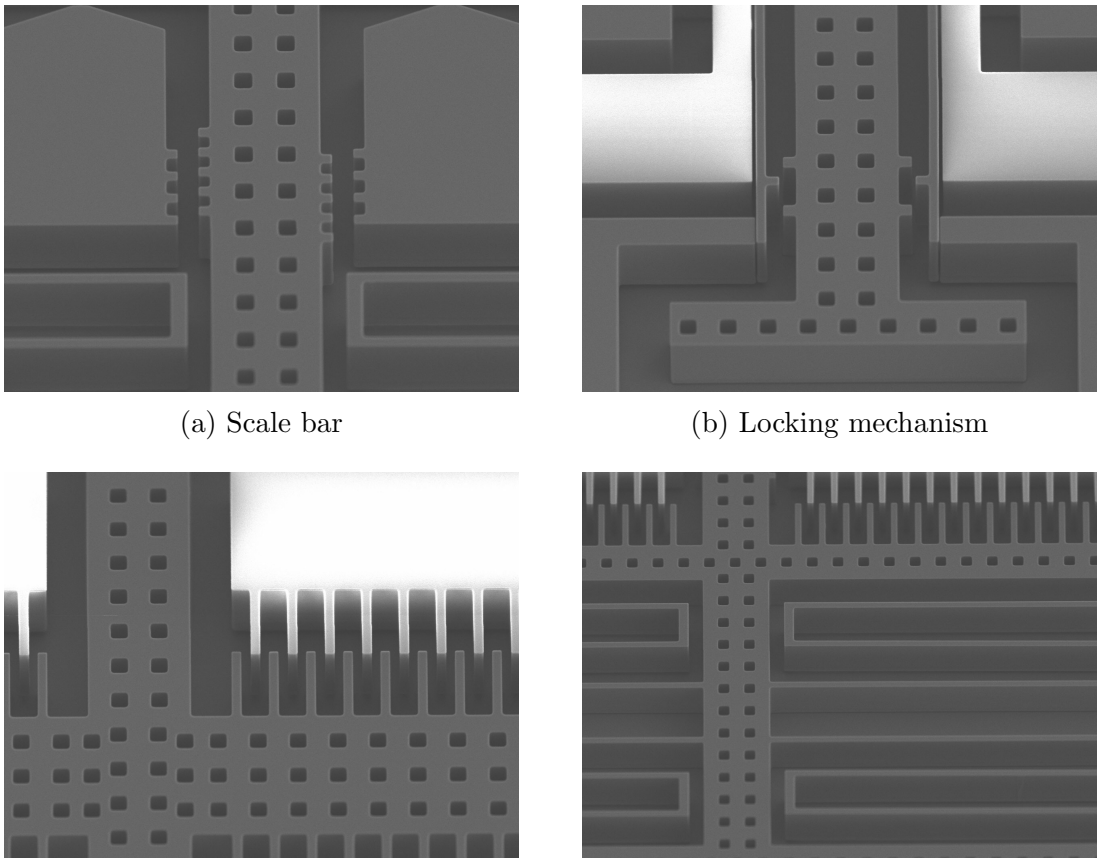

(a) Scale bar

(b) Locking mechanism

(c) Comb fingers

(d) Spring system

Figure 10: SEM images displaying different parts of the devices after fabrication.

After fabrication, the devices were inspected with LOM and SEM. Some of the moving structures started moving while looking in the SEM, which indicated successful release. Some moving structures displayed a focusing mismatch in the LOM, implying that they might be stuck. Figure 11b illustrates this observation, in which

the middle beam is in focus whereas the locking arms are not. Several measurements were made with the LOM in order to compare the fabricated geometry with the designed one. The distances measured can be seen in figure 11a. Table 1 shows a comparison of the designed length with the fabricated length of the six measurements in figure 11a. From these numbers it can be seen that the deviation is within $\pm 1\,\mu m$. In addition, it is noticeable that the geometries with more etched space around them were fabricated smaller than designed, whereas the ones with less space tended to be larger than designed.

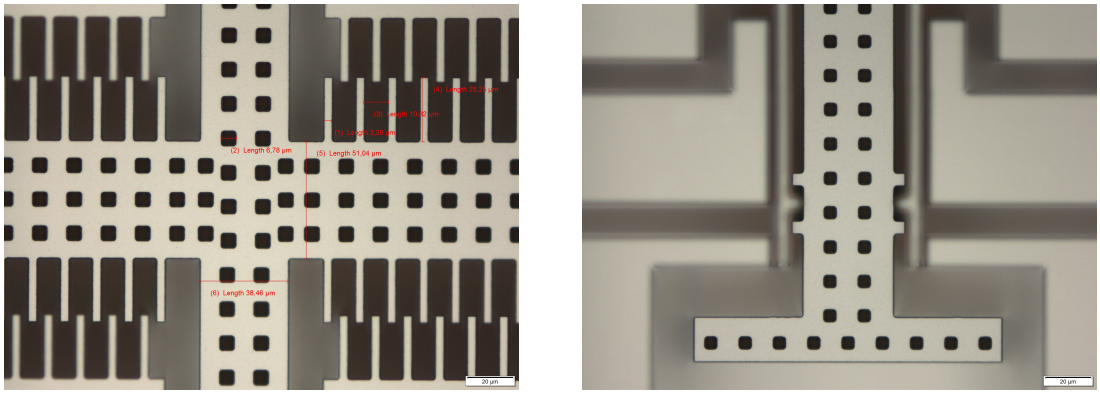

(a) LOM measurements (b) Focusing mismatch

Figure 11: LOM images showing several features after fabrication.

Table 1: Comparison between designed and fabricated features of the devices.

Feature #	**Designed** [µm]	**Fabricated** [µm]	Δ [µm]
1	4	3.26	0.74
2	6	6.78	-0.78
3	10	10.82	-0.82
4	28	28.25	-0.25
5	52	51.04	0.96
6	39	38.46	0.54

3 Device characterization

After fabrication the performance of the devices were evaluated. The performance of an actuator was divided into the following features:

- Electrostatic actuation of the comb drive.
- Mechanical actuation of the comb drive (if electrostatic did not work).
- Electrostatic actuation of the locking mechanism.

The categories above were used to benchmark if a device was functional. Each device was first tested electrostatically, this was done by mounting a chip onto the probing station and establish contact between the probes and the contact pads of the device. A voltage supply applied the actuation voltage and the movement of the comb was observed with the help of a microscope. With the built-in scale the distance of the movement was noted as well as the applied voltage for the specific distance. A fully functional device was defined as a device in which all of the tested features functioned as expected, and the function was reproducible. For designs A and B only the first two features were tested as there were no locking mechanism. The first feature to be evaluated was the electrostatic actuation. If a device displayed a satisfactory electrostatic actuation it directly passed the mechanical criteria automatically as the electrostatic force generated is significantly lower compared to the mechanical force while poking. A device was declared as fully functional if the electrostatic actuation was reproducible. A device that that was not able to actuate electrostatically was subjected to mechanical actuation. The criteria required for a device to pass as mechanically functional was that the comb and the spring were able to actuate and responded as intended when physically poking the comb with one of the probes, a device that only fulfilled the mechanical functionality was declared as partly functional.

Designs C and D required to be tested with two voltage supplies, one for the main actuator and the other for the locking mechanism as these designs had locking mechanism which would otherwise prohibit a full motion range of the comb. Design C and D could only be categorized as fully functional if the main actuator worked well in conjunction with the locking mechanism actuator, If only one actuation mechanism were working as intended it was declared partly working.

Design A was further tested with function generator to evaluate if the design was able to respond to various voltage functions such as wave, step and etc at different frequencies. Design A was chosen due to it being the most rigid design without a locking mechanism.

4 Results

4.1 Yield

Devices from several chips were tested in order to investigate possible differences in the fabrication. Figure 12 shows the yield of the devices. Figure 12a shows the results from testing only the comb drive in devices 1A and 1B. Figure 12b shows the results from testing comb drive and locking mechanism in devices 1C and 1D. The yield of fully functional devices for the main design was roughly 15% when only testing the actuation and roughly 25% when testing both actuation and locking mechanism. For the secondary design, none of the devices were fully functional when only the actuator was tested, though most of them were partially functional, i.e. moved when actuated. Almost half of the devices did not work at all when both comb drive and locking mechanism was tested, and none of them were fully functional. This is likely due to the inferior rotational stability of the secondary design, which was manifested in unstable movement and "hooking" to adjacent structures. In total, 32 devices were tested without the locking mechanism, of which 14 were of design 1A and 7 of design 1B. 15 devices were tested with both comb drive and locking mechanism, of which 11 were of design 1C and 4 were of design 1D. The most common reason why the devices were noted as "not functional" was that the movable parts were stuck and could not be released. The common reasons for "partly functional" were that the locking mechanism opened but did not close, that only one of the locking arms worked, or that the movable structure got stuck due to lateral or rotational instability. 3 devices of design 1C1 were tested, of which 2 were not functional, and 1 could not be actuated but the lock was able to partially close and open.

4.2 Simulations vs. fabricated devices

Comparing the manufactured devices with the simulations displayed as expected various differences. One of the most noticeable things was that the real world locking mechanism required significantly lower voltage, a mean of 28.5 V to fully open, compared to the calculated required voltage of 65 V. This could be due to not fully taking pull in into account when designing the lock, as it is basically almost a parallel plate actuator and that pull in would occur after it moved 1/3 of the initial gap. Another reason this might have been the case is that the locking cantilevers were a bit under etched and lost some of its mechanical stability leading to pull in.

Several of the design parameters like rotational and lateral stability were not possible to extract from the characterization, therefore the values for real device vs simulated cannot be compared. However, designs B and D (secondary) were clearly

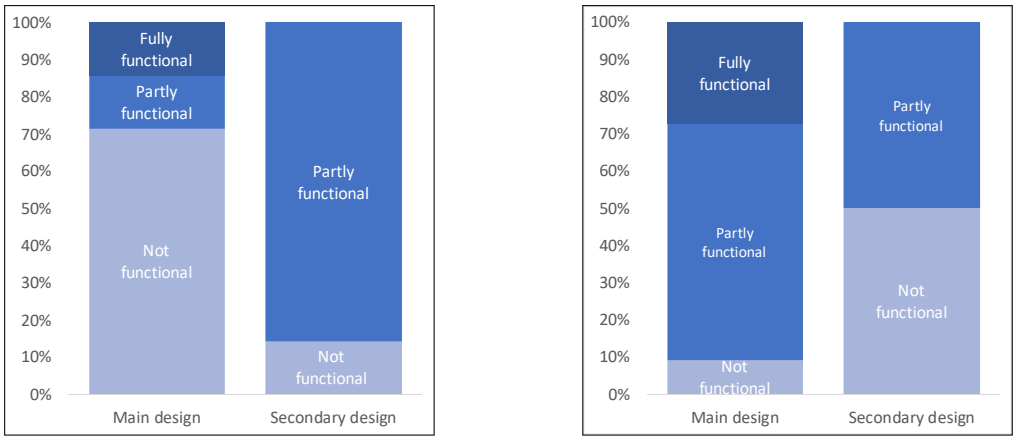

(a) Devices 1A & 1B.

(b) Devices 1C & 1D.

Figure 12: Yield of the tested devices.

less rigid and stable, as expected. This could be seen as the system started to rotate for voltages above 50 V. This was not the case for the main design.

4.3 Discussion

The grown version of the design should have been specified as the added 0.5 µm made the locking mechanism non-functional as the main actuator could not move past the locking cantilever even when actuated. This resulted in a actuation more than 6 µm in either direction was not possible before it got stuck. Design B had some major issues as 7/10 devices per chip had big rectangular blocks were the springs were supposed to be. The error must have occurred in AutoCAD when the devices were put onto the chip layout as some of the devices were imported as blocks while other was copy pasted. Unfortunately this error slipped through even though the K-layout file was examined before submission.

The main design actually worked quite well as we got a few fully functioning devices, the yield could always be improved. One problem that we realised while using the function generator was that the device had trouble getting rid of the charges building up. It would work for a couple of cycles then suddenly stop due to charges building up. This could be improved in future designs by making the transfer of charges more efficient.

A comparison was made between the fabricated device and the calculated behaviour based on force calculations for a comb drive actuator. The movement of the device was analyzed by applying an even interval of voltages and measuring the

displacement using the fabricated scale. In figure 13a, it is evident that although displaying a behaviour similar to that of the theoretical movement of a comb drive actuator with a spring constant of $1.74\,\mathrm{N\,m^{-1}}$, the absolute values are not in agreement. This is most likely not an effect of the resolution of the scale being too low, leading to measurement errors. Rather, it seems that the simulated spring constant of the restoring mechanism is not in agreement with that of the fabricated one. The data points represented on the evaluated values in the figure are those that were measured during evaluation.

An attempt was made to investigate this discrepancy by comparing the measured values with the theoretical movement of the same comb drive actuator but with different spring constants of the restoring mechanism. This comparison can be seen in figure 13b. From the figure, it can be seen that the measured values are in close agreement with a restoring mechanism of spring constant $k = 1.0\,\mathrm{N\,m^{-1}}$. Although this hypothesis can not be proven with the available data, it does provide some indication that the spring constant of the fabricated device might actually be lower than that of the simulated one.

It is also noticeable that the first data point with a non-zero value of displacement appears at an actuation voltage of 20 V. The actuator was not able to move the structure at voltages lower than that value, or at least not enough to be able to measure the displacement. This could be due to stiction.

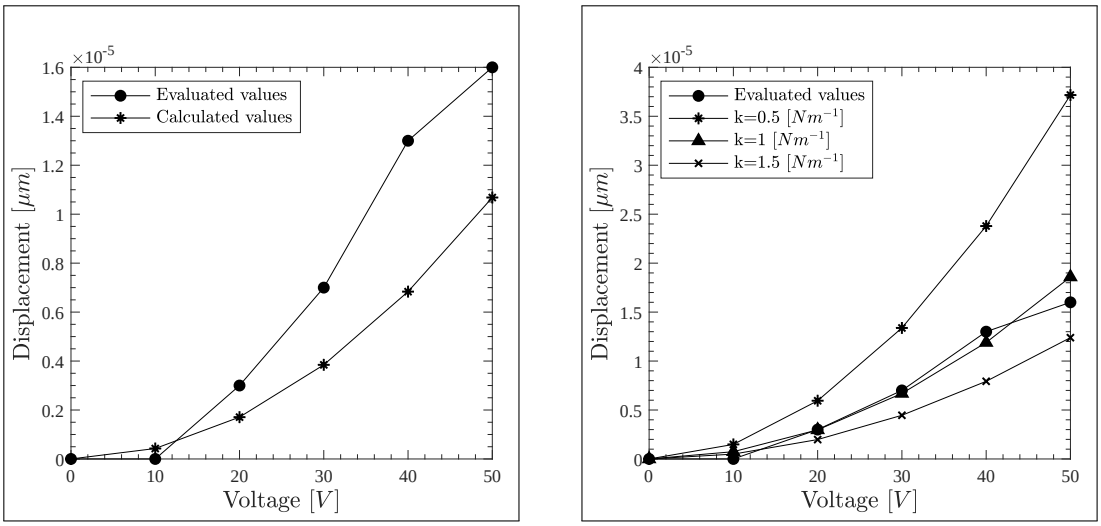

(a) At spring constant $k = 1.74\,\mathrm{N\,m^{-1}}$ (b) At different spring constants

Figure 13: Comparison between calculated values and the movement of device 1C.

5 Appendix

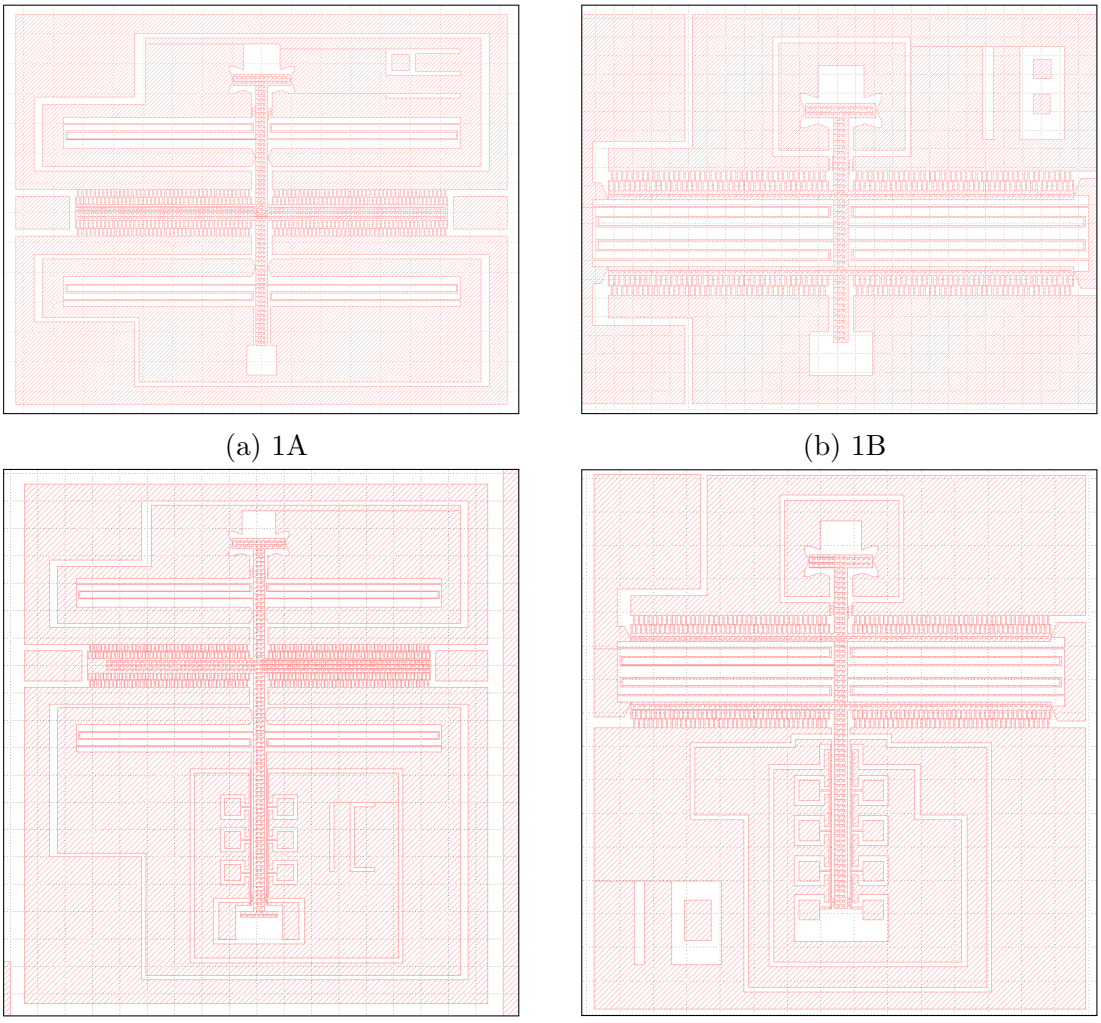

(a) 1A (b) 1B

(c) 1C (d) 1D

Figure 14: Finalized CAD drawing of the fabricated devices.